Mech. Sci., 11, 371–379, 2020
https://doi.org/10.5194/ms-11-371-2020

Mechanical Sciences
Open Access

Interfacial microstructures and properties of hyper-eutectic Al–21Si / hypo-eutectic Al–7.5Si bimetallic material fabricated by liquid–liquid casting route

Mohamed Ramadan[1,2] **and Abdulaziz S. Alghamdi**[1]

[1]Mechanical Engineering Department, College of Engineering, University of Ha'il, P.O. Box 2440 Ha'il, Saudi Arabia
[2]Central Metallurgical Research and Development Institute (CMRDI), Cairo, Egypt

Correspondence: Abdulaziz S. Alghamdi (a.alghamdi@uoh.edu.sa)

Received: 24 March 2020 – Revised: 10 August 2020 – Accepted: 11 September 2020 – Published: 27 October 2020

Abstract. The bimetal casting process using the liquid–liquid technique was developed to produce a high-quality hyper-eutectic Al–21Si / hypo-eutectic Al–7.5Si alloy bimetal material. Microstructure and microhardness were investigated as a function of the time interval between pouring hypo-eutectic and hyper-eutectic alloys. A bimetal material was successfully fabricated using a liquid–liquid casting technique with a 10 s time interval in a permanent mould casting. A unique structure comprised of hyper-eutectic Al–21Si, hypo-eutectic Al–7.5Si and a eutectic interface of 70 µm thickness was obtained. This structure totally differs from that obtained using a higher time interval above 10 s that showed an imperfect interface bond due to the shrinkage cavity and formation of oxides. The hardness variation from the upper zone of 117.5 HV to the lower zone of 76 HV corresponded to the variation in Si and the content of other alloying elements. The proposed total solidification time control method is a promising approach for the successful fabrication of liquid–liquid bimetal material.

1 Introduction

Functionally graded materials (FGMs) are engineering materials whose properties change gradually with volume. Although metal and polymer matrix composites (MMCs) have a broad spectrum of property combinations required in a wide range of engineering applications, high cost, corrosion behaviour and product machinability limitation sources of reinforcing materials are still a problem associated with the development of MMCs (Oghenevweta et al., 2014; Algamdi et al., 2018; Parida et al., 2014; Sahoo et al., 2013; Ray et al., 2018; Nayak et al., 2019). Bimetallic materials fabricated though liquid–solid and liquid–liquid casting routes could be promising alternatives for metal and polymer matrix composites for a wide range of materials to be used for engineering applications due to their low cost and high gradient physical and mechanical properties (Ramadan et al., 2020a, b and c). Researchers are applying extensive effort in order to control the composition and microstructure across the components to design materials with graded properties (Parihar et al., 2018, and Wang et al., 2015). For lightweight, tough, wear-resistant and low-cost FGM, designers are working on composite structures composed of dissimilar materials (Zhao et al., 2019; Wróbel, 2011). The notable merit of such dissimilar alloys is that a smooth change in properties can be achieved by combining different constituent alloys together, such as 304 stainless steel surface layer and a cast iron base by Ramadan (2015), Ramadan (2018) and Ramadan et al. (2017), two different Al–Si alloys by Scanlan et al. (2005), a Babbitt-steel bimetal composite by Fathy et al. (2018) and an Al/Mg alloy by Li et al. (2019), Z. Jiang et al. (2018) and W. Jiang et al. (2016a). Moreover, the design of automotive spare parts comprises the use of dissimilar lightweight materials such as special steels, aluminium alloys and plastic matrix composites according to Lee et al. (2014). Bimetal casting is considered to be one of the most important manufacture techniques for the fabrication of functionally graded metallic materials. Techniques of bimetal casting are mainly classified into liquid–solid and liquid–liquid techniques according to Bykov (2011) and Ramadan et al. (2019). The

liquid–liquid technique is a relatively difficult technique for the fabrication of bimetals compared with the liquid–solid technique. In the liquid–liquid technique, two furnaces are needed for two different melting point alloys.

The interfacial structure of bimetal materials fabricated by liquid–solid or liquid–liquid techniques is the most important factor affecting the bond between a pair of metals. According to the aim of achieving a high-quality bond of FGMs using both bimetal casting techniques, much research has been done to develop bimetal casting to achieve a higher performance and a lower production cost. For example, Al–Mg bimetallic castings are fabricated through the liquid–solid technique and lost foam casting by Jiang et al. (2016b). Results show that the reaction layer between Al and Mg was significantly affected with an increasing volume of liquid (Mg) to volume of solid (Al).

High-chromium white cast iron (HCWCI) and carbon steel composite liner are produced using a liquid–liquid composition process by Xiao et al. (2012). A composite bimetal liner has been developed successfully using the lost foam casting process. An Mg–Al bimetal is successfully fabricated through a liquid–liquid compound casting process using a solid Zn interlayer by Jiang et al. (2018). The addition of the thin solid Zn interlayer prevented both liquid metals from directly mixing and also restrained the Mg–Al intermetallic formation. An Al–Al bimetallic composite is fabricated through lost foam casting using a solid Zn interlayer by Jiang et al. (2018). A uniform metallurgical bond interface is obtained between the Al and the A356 Al alloy.

Centrifugal casting and the Cast–Decant–Cast (CDC) process have been used for the fabrication of Al–Si alloy FGM pistons by Scanlan et al. (2005) and Chirita et al. (2008). The CDC process was developed to produce functionally gradient light alloys. In the CDC process, the first alloy is poured into a mould and allowed to partially solidify against the mould walls to form a solid layer of a required thickness. The remaining unsolidified liquid of the first metal is decanted, and the second alloy is then poured into the mould. Although centrifugal casting and the CDC process have an ability to fabricate FGMs, the achievement of perfect interface FGM pistons by controlling the process parameters is still difficult and ambiguous. The controlling of the solidified layer thickness of the first metal and the time interval between pouring the first liquid and the second liquid have not been reported in detail. Moreover, Kreider (1974) reported that the quality of bimetallic materials is mainly dependent on the structure and properties of the interface layer between the dissimilar alloys.

Therefore, the aim of the current work is to fabricate FGMs with a varying gradient of high wear and temperature resistance and high machinability as well as toughness in the skirt region to be suitable for the application of automotive pistons. The effect of the time interval between pouring the first liquid and second liquid on achieving a perfect interface of hyper-eutectic Al–21 % Si and hypo-eutectic Al–7.5 % Si using gravity metallic mould casting is investigated.

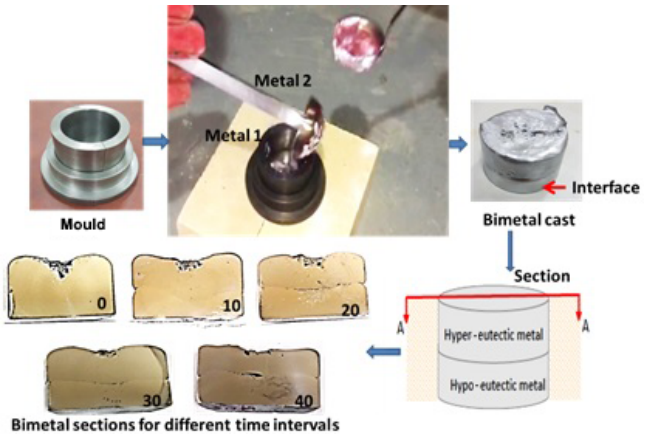

Figure 1. Schematic illustrating the layout of the mould, molten bimetal casting and sectioning of bimetal casting for different time intervals.

2 Material and methods

The raw materials used to fabricate both metals in the current study were Al–25 % Si master alloy, pure Cu, pure Al, reused automotive pistons and 6061 Al alloy. The chemical composition of both fabricated metals used in this study is shown in Table 1. Both metals were melted in two different conical graphite crucibles using an electrical furnace at a temperature of 750 °C and are held in the furnace for 30 min. One furnace was used for both metals due to their similar melting points.

The ratio of liquid 1 to liquid 2 in current bimetal casting was 1 : 1. Firstly, 140 g molten metal of hypo-eutectic Al–7.5Si was poured at a temperature of 720 °C into a flame-dried metallic mould (∼ 30 °C). Secondly, after certain time intervals (0–40 s), 140 g molten metal of hyper-eutectic Al–21Si was poured at a temperature of 720 °C into the mould containing the first metal. After solidification, the bimetal specimen was longitudinally sectioned and prepared for interfacial characterization. Figure 1 shows a schematic illustration of the metallic mould, pouring of the bimetal casting and longitudinal sectioning of bimetal castings for different time intervals.

For investigating the interface microstructure, specimens were cut, ground, polished and etched with a solution containing 0.5 % HF (hydrofluoric acid) + 99.5 % H_2O. For microstructure observations, an optical microscope connected with an advanced digital camera was used. Interface microstructures were observed with a scanning electron microscope (SEM), and the chemical compositions of the interface were also characterized through energy-dispersive X-ray spectroscopy (EDS) analysis. Microhardness tests were per-

Table 1. Chemical compositions of the materials (wt %).

Materials	Chemical compositions (wt %)								
	Si	Cu	Mg	Ni	Fe	Zn	Ti	Mn	Al
Hyper-eutectic Al–21Si	21.1	0.60	0.87	1.99	0.61	0.07	0.07	0.09	Bal.
Hypo-eutectic Al–7.5Si	7.48	0.94	0.22	0.09	0.71	0.09	0.06	0.01	Bal.

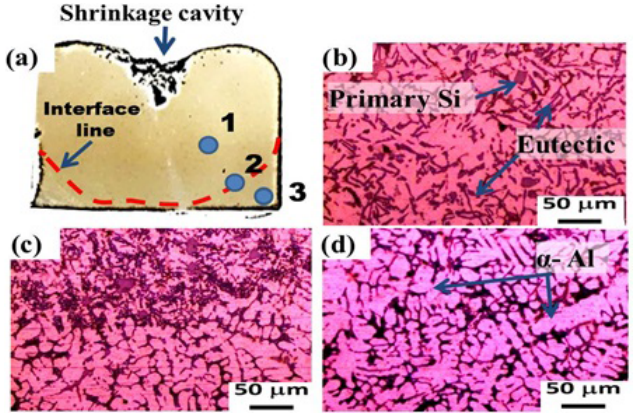

Figure 2. Macro- and microstructure of bimetal casting for a 0 s time interval. **(a)** Macrophotograph cross section. **(b, c, d)** Representation of the microstructures of points 1, 2 and 3, respectively.

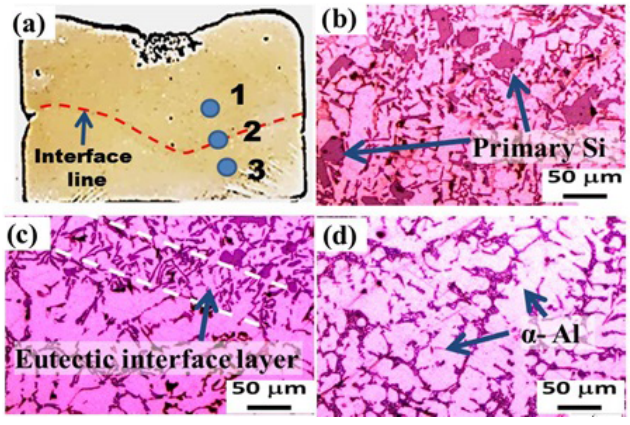

Figure 3. Macro- and microstructure of bimetal casting for a 10 s time interval. **(a)** Macrophotograph cross section. **(b, c, d)** Representation of the microstructures of points 1, 2 and 3, respectively.

formed using 0.25 kgf (kilogram force; 2.452 newton) loads, and the hardness value was taken from the average of five points measured in each specimen.

3 Results and discussion

Aluminium–silicon alloys are mostly multilateral materials; they make up a high percentage of the total aluminium alloy cast parts produced for the automotive industry. The presence of silicon in Al alloys reduces the thermal expansion coefficient, increases corrosion and wear resistance and improves casting and machining processing of the Al alloys. Depending on the percentage of Si in the Al–Si alloys, the solidification of hypo-eutectic or hyper-eutectic compositions starts with the primary α aluminium forms and grows in dendrites or silicon phase forms and grows in angular primary particles. By reaching the eutectic point, the fine eutectic (α+ Si) phases nucleate and grow until the end of solidification, as obtained by Bykov (2011).

The macro- and microstructure of Al–Si bimetal material for a 0 s time interval are shown in Fig. 2. The hypoeutectic structure (as shown in Fig. 2d, point 3) consists of primary aluminium α phase and fine eutectic silicon phase. Hyper-eutectic alloys with a near-eutectic structure containing a lower percentage of coarse, angular primary silicon particles and fine eutectic silicon phase are observed on the interface (point 2) and on the zone above the interface (point 1) (see Fig. 2b, c).

Pouring liquid metal of Al–20Si directly after pouring liquid metal of Al–7.5Si without a time interval (0 s) promotes the formation of a new Al–Si alloy due to the complete solubility of Si in Al in a liquid state. A hyper-eutectic alloy with a near-eutectic structure is obtained for most of the bimetal structure area. A few areas of hypo-eutectic structure are observed due to the higher solidification rate of higher temperature liquid metal poured in the metallic mould of a lower temperature.

By applying a 10 s time interval between pouring the first liquid Al–7.5Si and second liquid Al–21Si, two clearly different microstructures of hyper-eutectic Al–Si alloy and hypo-eutectic alloy separated by eutectic structure alloy are obtained, as shown in Fig. 3. It is obvious that applying a 10 s time interval between the first liquid metal and second liquid metal facilitates the formation of a considerable solidified zone of the first poured liquid metal. A smooth change in the microstructure from hyper-eutectic to eutectic and then to a hypo-eutectic structure is observed. Therefore, a eutectic structure interface layer with a thickness of approximately 70 µm can be achieved by applying a time interval of 10 s.

The macro- and microstructure of bimetal casting for a 20 s time interval are shown in Fig. 4. It is observed that an interfacial bonded area of bimetal is performed only on the outer surface of specimens. In the centre of the bimetal

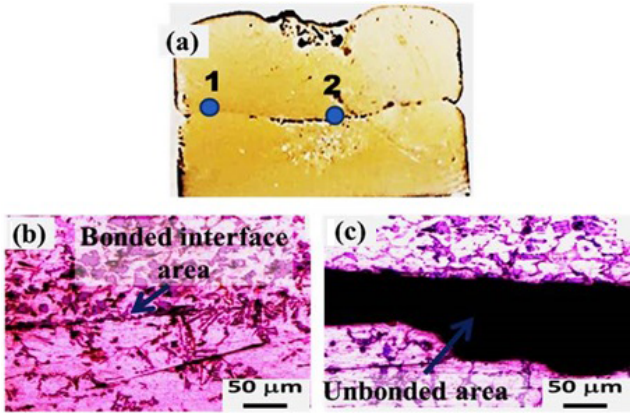

Figure 4. Macro- and microstructure of bimetal casting for a 20 s time interval. **(a)** Macrophotograph cross section. **(b, c)** Representation of the microstructures of points 1 and 2, respectively.

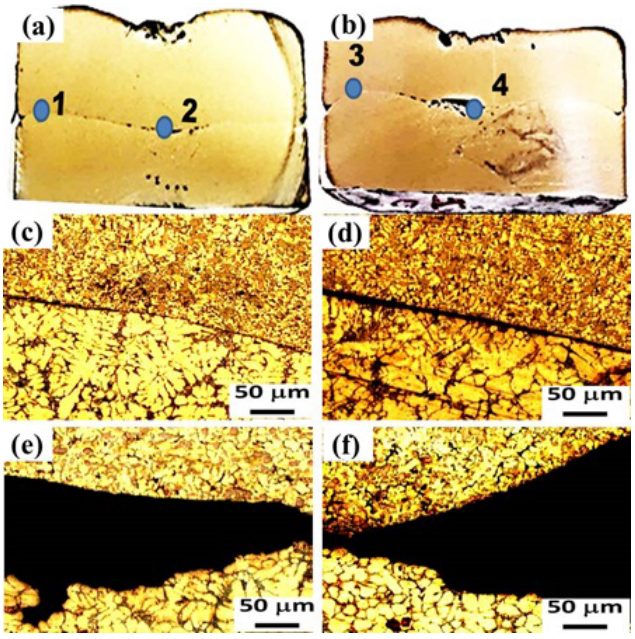

Figure 5. Macro- and microstructure of bimetal casting for 30 and 40 s time intervals. **(a)** Macrophotograph cross section for a 30 s time interval. **(c, e)** Representation of the microstructures of points 1 and 2, respectively.**(b)** Macrophotograph cross section for a 40 s time interval. **(d, f)** /microstructures of points 3 and 4, respectively.

specimens, unbonded interface areas are observed. Transformation from a liquid to a solid state is often accompanied by a decrease in volume. For particular aluminium alloys, it was found that the tendency for shrinkage porosity formation is mainly related to the liquid–solid volume fraction and the solidification temperature range of this Al alloy (ASM International, 2008).

Shrinkage cavity often results from the loss of volume during solidification. This type of volume contraction is highly affected by different processing parameters, such as volume total cooling surface area, pouring temperature and moulding materials. To eliminate shrinkage cavity that formed in liquid–liquid bimetal gravity casting, the riser for the second metal is usually designed and placed at the top of the second metal to supply liquid to the system through the force of gravity. The riser should be designed to ensure that molten metal inside the riser solidifies at the end of the solidification process. For the first poured liquid metal, shrinkage can be eliminated or compensated for by the second poured metal after a certain time interval. Future research of our research team will focus on this parameter to optimize risering for bimetal casting (Tijani et al., 2013; Chen et al., 2019). An unfused defect is in most cases oxide skins that are generated during casting of Al alloys. This Al_2O_3 oxide thin layer of the first liquid is believed to break because of surface turbulence of the second poured liquid metal in liquid–liquid bimetal casting.

By increasing the time interval to 30 and 40 s as shown in Fig. 5, the unbonded area of the bimetal interface for both the outer surface and centre of specimens increases. As for 20, 30 and 40 s time intervals, a perfect interface and metallic bond have not been achieved. A previous study by Rahvard et al. (2014), in which A390/A356 bimetallic Al alloys were fabricated through the CDC process, reported that a short time between decanting and pouring the second alloy must be applied to achieve a good metallic bond bimetal interface without the formation of oxide film and/or shrinkage cavity. The formation of oxide surfaces can be increased by increasing the time interval. Dispinar et al. (2010) reported that oxide surfaces almost have an unbonded area and air gap in-between that may disband and open up, causing porosity during solidification. For the second metal (hyper-eutectic structure) that exists on the top of the bimetal cast, the riser could be applied to compensate for the volume contraction and prevent shrinkage cavity formation.

The oxidation of hyper-eutectic Al–21 % Si and hypo-eutectic Al–7.5 % Si alloys is a very important phenomenon that affects the quality of the interface bond in compound casting. For the solid–liquid casting route, Al solid substrate should be carefully prepared by using grinding papers and a stronger flux to remove Al oxide from the surface as well as using an intermediate layer before pouring the second molten metal. In liquid–liquid casting, as in the current study, a lower superheating temperature, alloy chemistry (addition of Cu, Ni, Fe, etc.) and controlled furnace atmosphere (Argon gas) affected dross formation and minimized the oxidation of Al alloys used (Tijani et al., 2013; Chen et al., 2019). Also, reducing unnecessary holding time in the furnace, reducing door openings and decreasing the pouring rate can avoid excess oxidation. Beside the processing melting and casting control, the oxide formation on the outer surface of the first poured metal is highly affected by the time interval.

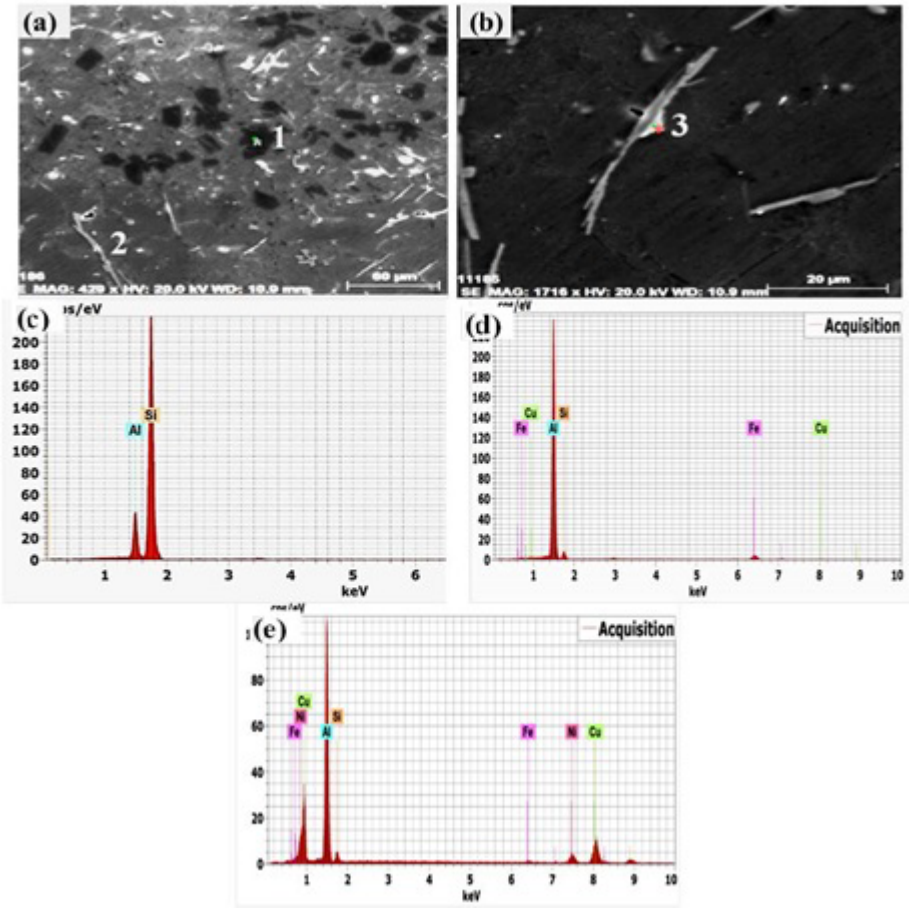

Figure 6. Microstructural analysis and EDS microanalysis data of bimetal casting with a 10 s time interval. **(a, b)** SEM micrographs. **(c, e)** EDS microanalysis data of points 1 and 3 in the hyper-eutectic region and **(d)** EDS microanalysis data of point 2 in the hypo-eutectic region.

When using a lower time interval up to 10 s, the interface oxide formation is not observed.

More investigations have been conducted on the bimetal casting alloy that was fabricated using a 10 s time interval between pouring the hypo-eutectic and hyper-eutectic structure Al alloys. Figure 6 shows the microstructural analysis and EDS microanalysis data of bimetal casting with a 10 s time interval. Microstructural analysis and EDS microanalysis confirm the presence of different phases in typical hyper-eutectic, eutectic and hypo-eutectic structures of bimetal. Hypereutectic Al–Si alloys that usually contain coarse primary silicon particles (PSPs) are detected as shown in Fig. 6a and c (point 1). Intermetallic precipitates due to alloying with Fe, Cu and Ni are observed, as shown in Fig. 6a, b, d and e (points 2 and 3).

The microstructural characteristics and elements' line scan analysis through the interface of bimetal casting for a 10 s time interval are shown in Figs. 7 and 8. The prevailing element diffused gradually in the transition area from the upper hyper-eutectic structure Al alloy zone that is rich in Si (21 %) to the lower hypo-eutectic structure that is poor in Si (7.5 %). The interface transition area shows a new microstructure characteristic containing finer eutectic and primary Si due to the higher solidification rate adjacent to the solidified layer as shown in Figs. 7 and 8. Eutectic transition width can be easily detected by microstructure and elements' line scan analysis. The bimetal specimen fabricated with a 10 s interval shows a perfect interfacial area that formed due to the formation of eutectic structures that are due to a mixture of hyper- and hypo-eutectic structures' formation. Al–Si alloys with 12 to 13 pct Si are almost completely Al–Si eutectic at the end of solidification. Here in liquid–liquid bimetal casting, the solidification structure of the interface is highly affected by the chemical composition of both metals used as well as the interfacial cooling rate. An interfacial microstructure that is purely eutectic, α-Al+ eutectic or primarily Si+ eutectic could be achieved, depending on chemical composition and both of the metals' casting total solidification time. In general, the fine grain structure is preferred in Al–Si alloy castings with eutectic or near-eutectic structure to improve

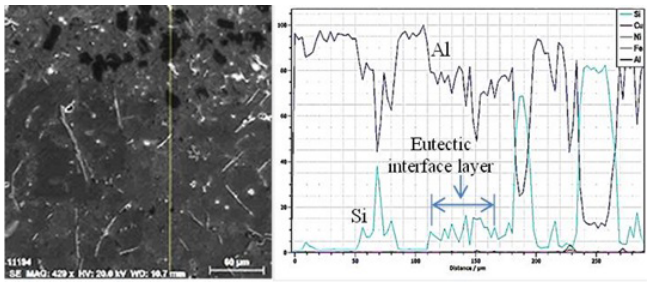

Figure 7. Interface elements' line scan analysis of bimetal casting for a 10 s time interval.

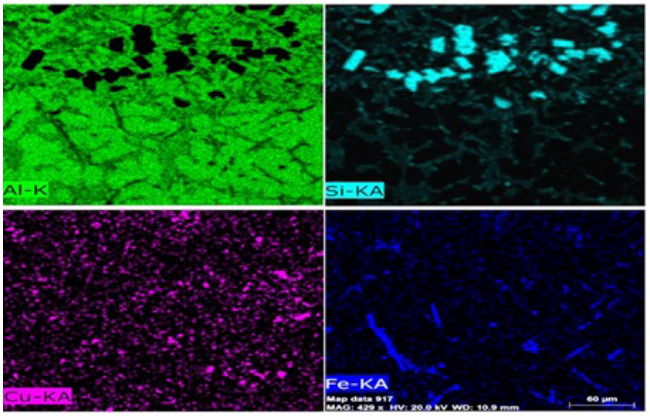

Figure 8. Concentration mappings of Al, Si, Cu and Fe in Fig. 7a of the bimetal casting interface using a 10 s time interval.

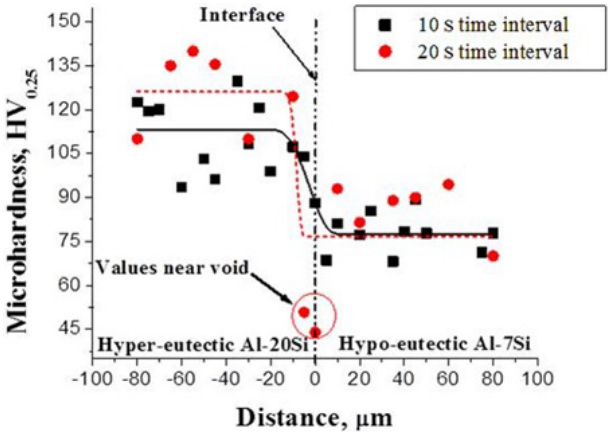

Figure 9. Variations in Vickers microhardness values from hyper-eutectic Al–21Si to hypo-eutectic Al–7Si for two different time intervals.

their resistance to hot tearing, mechanical properties and surface finishing characteristics (Tiedje et al., 2012).

During the solidification of liquid hypo-eutectic Al–7.5Si, the α-Al present in the Al–7.5Si alloy starts solidifying by rejecting the Si into the liquid melt from the solidification front. The entire melt of the Al–7.5Si Al alloy will solidify within its total solidification time after pouring. The hyper-eutectic Al–21Si alloy is poured over the hypo-eutectic Al–7.5Si alloy at 720 °C 10 s after the pouring of the hypo-eutectic Al–7.5Si alloy. As soon as the Al–21Si liquid melt comes in contact over the partially solidified Al–7.5Si alloy, it intermixes with the remaining Al–7.5Si liquid.

Here the total solidification time of the first poured liquid metal in liquid–liquid bimetal casting is a very important factor to achieve a good interfacial bonding area. By calculating the total solidification time of the first liquid metal, the time interval between pouring the first liquid metal and the second one could be controlled. The amount of solidified metal of first poured liquid metal could be controlled by selecting a suitable time interval that should be slightly less than its total solidification time. In the current work the total solidification time of 14–17 s for the first poured liquid hypo-eutectic Al–7.5Si alloy is calculated using Chvorinov's rule (see Eqs. 1 and 2) and its modification, considering shape, size and the superheat effect according to Tiryakioglu et al. (1997) and Groover (2010). In the current research work the constant n (power of modulus (V/A)) is estimated to be 1 depending on using a small permanent mould casting according to Tiryakioglu et al. (1997) and Campbell (1991).

$$t = B\left(\frac{V}{A}\right)^n \tag{1}$$

$$B = \left[\frac{\rho_m L}{(T_m - T_o)}\right]^2 \left[\frac{\pi}{4k\rho c}\right]\left[1 + \left(\frac{c_m \Delta T_s}{L}\right)^2\right], \tag{2}$$

where V is the volume of cast, A is the total surface area of cast, B is the mould and metal constant ($s\,m^{-2}$), T_m is the melting temperature of the liquid (K), T_o is the temperature of the mould (in K), ΔT_s is superheat (K), L is latent heat of fusion ($J\,kg^{-1}$), k is the thermal conductivity of the mould ($W\,m^{-1}\,K^{-1}$), ρ is the density of the mould ($kg\,m^{-3}$), c is the specific heat of the mould ($J\,kg^{-1}\,K^{-1}$), ρ_m is the density of the metal ($kg\,m^{-3}$) and c_m is the specific heat of the metal ($J\,kg^{-1}\,K^{-1}$).

By using 10 s time intervals, some of the remaining liquid of the first metal and the new hyper-eutectic alloy are mixed in the area of interface causing intermingling of the two alloys that forms a eutectic or near-eutectic interface structure. A perfect interfacial structure could be achieved in liquid bimetal material casting using a time interval that is lower by a few seconds (4–7) than the solidification time of the first poured liquid metal.

Variations in Vickers microhardness values from hyper-eutectic Al–21Si to hypo-eutectic Al–7Si for 10 and 20 s time intervals are shown in Fig. 9. The figure shows that the hardness variation from the upper zone of 117.5 HV (average value) to the lower zone of 76 HV (average value) corresponds to the variation in Si and other alloying elements' content. For the interface transition layer of a 10 s time interval, the hardness shows a near to average value that is related

to the fine microstructure of Si and eutectic formation. On the other hand, the hardness shows a relatively lower value of 45.5 HV for the interface transition layer of a 20 s time interval that is due to the effect of shrinkage cavity formation.

Based on the current work experiments and results, it is concluded that the current liquid–liquid casting process has the ability to fabricate a hyper-eutectic Al–21Si / hypo-eutectic Al–7.5Si alloy bimetal material with a perfect interfacial area using a 10 s time interval. The liquid–liquid bimetal casting process in a closed mould is a technology that mainly depends on a gating system design in which two independent gating systems are used for the filling of the mould cavity (Ramadan et al., 2019). Other important factors besides the time interval that affect the liquid–liquid casting process are metals' volume, cooling surface area, metals' composition and moulding materials. The novel solidification time approach that is proposed by the current study can collate all previous factors into one factor to successfully achieve a high-quality liquid–liquid bimetal casting product. Using a total solidification time control method is a promising approach for the successful fabrication of liquid–liquid bimetal materials, whereby the solidification layer of the first poured liquid metal could be controlled by estimating the time interval to be slightly less than the total solidification time of the first poured liquid metal.

4 Conclusions

1. A hyper-eutectic Al–21Si / hypo-eutectic Al–7.5Si alloy bimetal material was successfully fabricated using a liquid–liquid configuration gravity permanent mould casting process with a 10 s time interval.

2. The Al–7.5Si liquid, which was poured into the mould first, served as the substrate for the Al–21Si liquid. A eutectic structure interface layer with a thickness of approximately 70 µm was achieved by applying a time interval of 10 s.

3. The liquid–liquid configuration gravity permanent mould casting process with 0 s and 20 s time intervals and higher showed an imperfect interface bond due to either liquid–liquid alloying, as for a 0 s time interval, or shrinkage cavity and the formation of oxides, as for a 20 s time interval or higher.

4. The most suitable time interval for liquid–liquid bimetal material casting is mainly dependent on the solidification time of the first poured metal.

5. The variation in the hardness values from the upper zone of 117.5 HV to the lower zone of 76 HV is proposed to be linked to the variation in Si and the other alloying elements' content.

Data availability. All data included in this study are available upon request by contacting the corresponding author.

Author contributions. MR and ASA contributed equally to the research work in designing and conducting the study, analysing the data and writing the manuscript.

Competing interests. The authors declare that they have no conflict of interest.

Acknowledgements. The present research work has been undertaken within the funded research projects of the University of Ha'il, Kingdom of Saudi Arabia (Deanship of Scientific Research RG-191193).

Financial support. This research has been supported by the Research Deanship at the University of Ha'il (grant no. RG-191193).

Review statement. This paper was edited by Kheng Lim Goh and reviewed by three anonymous referees.

References

Algamdi, A. S., Ramadan, M., Abdel Halim, K. S., and Fathy, N.: Microscopical Characterization of Cast Hypereutectic Al-Si Alloys Reinforced with Graphene Nanosheets, Eng. Technol. Appl. Sci. Res., 8, 2514–2519, 2018.

ASM International: ASM Handbook: V15 Casting, ASM International, USA, 2008, 1149–1164, 2008.

Bykov, A. A.: Bimetal production and applications, Steel in Translation, 41, 778–786, doi.org/10.3103/S096709121109004X, 2011.

Campbell, J.: Castings, 2nd Edn., Butterworth Heinemann, Oxford, United Kingdom, 223–339, 1991.

Chen, Q. and Griffiths, W. D.: The investigation of the floatation of double oxide film defect in liquid aluminium alloys by a four-point bend test, Int. J. Cast Metal. Res., 32, 221–228, https://doi.org/10.1080/13640461.2019.1635348, 2019.

Chirita, G., Soares, D., and Silva, F. S.: Advantages of the centrifugal casting technique for the production of structural components with Al-Si alloys, Material. Design, 29, 20–27, https://doi.org/10.1016/j.matdes.2006.12.011, 2008.

Dispinar, D., Akhtar, S., Nordmark, A., Sabatino, M. D., and Arnberg, L.: Degassing, hydrogen and porosity phenomena in A356, Mater. Sci. Eng. A, 527, 3719–3725, https://doi.org/10.1007/s11665-018-3534-0, 2010.

Fathy, N. and Ramadan, M.: Influence of volume ratio of liquid to solid and low pouring temperature on interface structure of cast Babbitt-steel bimetal composite, AIP Conference Proceedings, 1966, 020028, https://doi.org/10.1063/1.5038707, 2018.

Groover, M. P.: Fundamentals of Modern Manufacturing: Materials, Processes and Systems, Hoboken, NJ, John Wiley & Sons, Inc., 223 pp., 2010.

Jiang, W., Li, G., Fan, Z., Wang, L., and Liu, F.: Investigation on the interface characteristics of Al/Mg bimetallic castings processed by lost foam casting, Metall. Mater. Trans. A, 47, 2462–2470, 2016a.

Jiang, W., Fan, Z., Li, G., Yang, L., and Liu, X.: Effects of Melt-to-Solid Insert Volume Ratio on the Microstructures and Mechanical Properties of Al/Mg Bimetallic Castings Produced by Lost Foam Casting, Metall. Mater. Trans. A, 47, 6487–6497, 2016b.

Jiang, W., Li, G., Wu, Y., Liu, X., and Fan, Z.: Effect of heat treatment on bonding strength of aluminum/steel bimetal produced by a compound casting, J. Mater. Process. Tech., 258, 239–250, 2018a.

Jiang, W., Jiang, Z., Li, G., Wu, Y., and Fan, Z.: Microstructure of Al/Al bimetallic composites by lost foam casting with Zn interlayer, Mater. Sci. Technol., 34, 487–492, https://doi.org/10.1080/02670836.2017.1407559, 2018b.

Jiang, Z., Fan, Z., Jiang, W., Li, G., Wu, Y., Guan, F., and Jiang, H.: Interfacial microstructures and mechanical properties of Mg/Al bimetal produced by a novel liquid-liquid compound casting process, J. Mater. Process. Tech., 261, 149–158, https://doi.org/10.1007/s00170-018-2990-x, 2018.

Kreider, G. K.: Metallic Matrix Composite, 1st Edn., Composite Materials, Vol. 4, Academic Press, New York, London, p. 506, 1974.

Lee, C. J., Lee, J. M., Ryu, H. Y., Lee, K. H., Kim, B. M., and Ko, D. C.: Design of hole-clinching process for joining of dissimilar materials – Al6061-T4 alloy with DP780 steel, hot-pressed 22MnB5 steel, and carbon fiber reinforced plastic, J. Mater. Process. Tech. 214, 2169–78, https://doi.org/10.1007/s00170-015-7363-0, 2014.

Li, G., Jiang, W., Yang, W., Jiang, Z., Guan, F., Jiang, H., and Fan, Z.: New insights into the characterization and formation of the interface of A356/AZ91D bimetallic composites fabricated by compound casting, Metall. Mater. Trans. A, 50, 1076–1090, 2019.

Nayak, S., Nayak, R. K., Panigrahi, I., and Sahoo, A. K.: Tribo-Mechanical Responses of Glass Fiber Reinforced Polymer Hybrid Nanocomposites, Materials Today: Proceedings, 18, 4042–4047, 2019.

Oghenevweta, J. E., Aigbodion, V. S., Nyior, G. B., and Asuke, F.: Mechanical properties and microstructural analysis of Al-Si-Mg/carbonized maize stalk waste particulate composites, J. King Saud. Univ. – Eng. Sci., 28, 222–229, 2014.

Parida, A. K., Das, R., Sahoo, A. K., and Routara, B. C.: Optimization of cutting parameters for surface roughness in machining of gfrp composites with graphite/fly ash filler, Proc. Mater. Sci., 6, 1533–1538, 2014.

Parihar, R. S., Setti, S. G., and Sahu, R. K.: Recent advances in the manufacturing processes of functionally graded materials: a review, Sci. Eng. Compos. Mater., 25, 309–336, https://doi.org/10.1515/secm-2015-0395, 2018.

Rahvard, M. M., Tamizifar, M., Boutorabi, M. A., and Shiri, S. G.: Effect of superheat and solidified layer on achieving good metallic bond between A390/A356 alloys fabricated by cast-decant-cast process, Trans. Nonferrous Met. Soc. China, 24, 665–672, https://doi.org/10.1016/S1003-6326(14)63109-5, 2014.

Ramadan, M.: Interface characterization of bimetallic casting with a 304 stainless steel surface layer and a gray cast iron base, Adv. Mater. Res., 1120, 993-998, https://doi.org/10.4028/www.scientific.net/AMR.1120-1121.993, 2015.

Ramadan, M.: Interface Structure and Elements Diffusion of As-Cast and Annealed Ductile Iron/Stainless Steel Bimetal Castings, Engineering, Technol. Appl. Sci. Res., 8, 2709–2714, 2018.

Ramadan, M., Hafez, K. M., Abdel Halim, K. S., Fathy, N., Chiba, T., Sato, H., and Watanabe, Y.: Influence of Heat Treatment on Interface Structure of Stainless Steel/Gray Iron Bimetallic Layered Castings, Appl. Mechan. Mater., 873, 3–8, 2017.

Ramadan, M., Fathy, N., Abdel Halim, K. S., and Alghamdi, A. S.: New trends and advances in bi-metal casting technologies, Int. J. Adv. Appl. Sci., 6, 75–80, https://doi.org/10.21833/ijaas.2019.02.011, 2019.

Ramadan, M., Ayadi, B., Rajhi, W., and Alghamdi, A. S.: Influence of Tinning Material on Interfacial Microstructures and Mechanical Properties of Al12Sn4Si1Cu/Carbon Steel Bimetallic Castings for Bearing Applications, Key Engineering Materials, 835, 108–114, 2020a.

Ramadan, M., Subhani, T., Rajhi, W., Ayadi, B., and Alghamdi, A. S.: A Novel Technique to Prepare Cast Al-bearing alloy/Wrought Steel Bimetallic Specimen for Interfacial Shear Strength, Int. J. Eng. Adv. Technol., 9, 3322–3326, 2020b.

Ramadan, M., Alghamdi, A. S., Subhani, T., and Abdel Halim, K. S.: Fabrication and Characterization of Sn-Based Babbitt Alloy Nanocomposite Reinforced with Al2O3 Nanoparticles/Carbon Steel Bimetallic Material, Materials, 13, 2759, https://doi.org/10.3390/ma13122759, 2020c.

Ray, S., Rout, A. K., and Sahoo, A. K.: Development and characterization of glass/polyester composites filled with industrial wastes using statistical techniques, Indian J. Eng. Mater. Sci., 25, 169–182, 2018.

Sahoo, A. K. Pradhan, S., and Rout, A. K.: Development and machinability assessment in turning Al/SiCp-metal matrix composite with multilayer coated carbide insert using Taguchi and statistical techniques, Archiv. Civil Mechan. Eng., 13, 27–35, 2013.

Scanlan, M., Browne, D. J., and Bates, A.: New casting route to novel functionally gradient light alloys, Mater. Sci. Eng. A, 413/414, 66–71, https://doi.org/10.1016/j.msea.2005.09.004, 2005.

Tiedje, N. S., Taylor, J. A., and Easton, M. A.: Feeding and Distribution of Porosity in Cast Al-Si Alloys as Function of Alloy Composition and Modification, Metall. Mater. Trans. A, 43, 4846–4858, 2012.

Tiryakioglu, M., Tiryakioglu, E., and Askeland, D. R.: Statistical Investigation of the Effects of Shape, Size and Superheat on Solidification Times of Castings, AFS Transactions 95, 907–913, 1997.

Tijani, Y., Heinrietz, A., Stets, W., and Voigt, P.: Detection and Influence of Shrinkage Pores and Nonmetallic Inclusions on Fatigue Life of Cast Aluminum Alloys, Metall. Mater. Trans. A, 44, 5408–5415, 2013.

Wang, G., Huang, H., Yang, Z., Shi, X., and He, X.: Numerical Simulation on the Die Filling Process of the Thixo-Forging of Al-7 wt pct Si/Al-22 wt pct Si Bimetal Composite, Metall. Mater. Trans. B, 46, 2121–2128, https://doi.org/10.1007/s11663-015-0404-0, 2015.

Wróbel, T.: Bimetallic layered castings alloy steel–grey cast iron, Archiv. Mater. Sci. Eng., 48, 118–125, 2011.

Xiao, X., Ye, S., Yin, W., and Xue, Q.: HCWCI/Carbon Steel Bimetal Liner by Liquid-Liquid Compound Lost Foam Casting, J. Iron Steel Res. Int., 19, 13–19, https://doi.org/10.1016/S1006-706X(12)60145-9, 2012.

Zhao, J., Zhao, W., Qu, S., and Zhang, Y.: Microstructures and mechanical properties of AZ91D/0Cr19Ni9 bimetal composite prepared by liquid-solid compound casting, Trans. Nonferrous Met. Soc. China, 29, 51–58, https://doi.org/10.1016/S1003-6326(18)64914-3, 2019.